Revista de Chimie
https://revistadechimie.ro
https://doi.org/10.37358/Rev.Chim.1949

Recycling of Steel Industry Waste Acid in the Preparation of Fe_3O_4 Nanocomposite for Heavy Metals Remediation from Wastewater

NAGY A.E. EMARA[1], REHAB M. AMIN[1], AHMED F YOUSSEF[2], SOUAD A. ELFEKY[1]*
[1]Department of Laser Applications in Metrology, Photochemistry, and Agriculture, National Institute of Laser Enhanced Sciences, Cairo University, Giza, 12613, Egypt
[2]Chemistry Department, Faculty of Science, Cairo University, Giza 12613, Egypt

Abstract. *This study was steered to convert waste acid ensued from the pickling process in steel industries to an esteemed nanocomposite for the elimination of heavy metals (HMs) from wastewater. Magnetic nanoparticles (Fe_3O_4) preparation from waste was performed by the co-precipitation method. These magnetic nanoparticles are modified by carboxymethyl-β-cyclodextrin polymer (CM-β-CD) through copolymerization reactions. The data obtained from FTIR, XRD, and TEM point up that CM-β-CD is entrenched onto Fe_3O_4 nanoparticles. The generated CM-β-CD / Fe_3O_4 was employed for HMs deportation from contaminated water and the adsorption results revealed that CM-β-CD/ Fe_3O_4 sorption efficiency was in the order of Pb(II) > Cd(II) > Cr(VI). The highest adsorption capacity was 64.2 (mg/g) for Pb(II). The kinetic study revealed that the HMs sorption by CM-β-CD/ Fe_3O_4 follows the pseudo-second-order model. The equilibrium modeling study proved that the Langmuir isotherm model was more fitting. The coexisting ions do not significantly alter the percentage removal of the measured metal ions. The efficiency of the synthesized polymer is particularly high in the tested field samples. Thus, CM-β-CD/ Fe_3O_4 has an extremely high adsorption capability in the field application as well as excellent reusability results, which will reduce the cost for the CM-β-CD / Fe_3O_4 as an adsorbent for wastewater treatment.*

Keywords*: Magnetic nanoparticles; Nanocomposite; Steel industry waste; Recycling; Heavy metals; Carboxymethyl-β-cyclodextrin*

1.Introduction

The fate and toxicity of chemicals in wastewater treatment plants are of great concern due to their direct and hazardous consequences on the environment and human safety [1].

Wastewater treatment is essential for industrial activities. The discharged wastewater from steel production processes like hot and cold rolling and hot-dip plating contain toxic HMs such as Pb(II), Cd(II), Ni(II), and Cr(VI) ions [2]. These ions have bad effects if they were used in crop irrigation, due to accumulation inside these crops. If it transfers to human livers, it will cause serious chronic diseases [3]. Benjamin A. Rybicki M.H.S. et al. [4] suggested a geographic association between Parkinson's disorder transience and the developed usage of HMs. José M. Matés et al. [5] explored various studies done on HMs effect on health. They declared that cadmium alters gene expression and signal transduction and diminishes activities of proteins implicated in antioxidant defense, prying with DNA repair and changing cancer progress and brain function. Cobalt aggravates the production of reactive oxygen species and DNA damage in cancer cells and brain tissue, changing propagation and differentiation and causing apoptosis. Copper plays a major role in cell division processes in both normal and tumor cells. Moreover, copper has a significant role in neurodegenerative diseases such as Parkinson's, Alzheimer's, and amyotrophic lateral sclerosis. Pierluigi E. Bigazzi [6] described that there is significant evidence that mercury can stimulate autoimmune disease in humans. Shikhar Agarwal et al. [7] observed that there is a significant association between composite cardiovascular and cerebro-

**email: dr_souad_elfeky@niles.edu.eg*

-vascular disease (CCVD) and urinary antimony, cadmium, cobalt, and tungsten. Great amounts of serum cadmium (>0.61 µg/L) were related to CCVD.

Due to the fatal effects and troubles caused by HMs accumulation in the environment, various methods have been developed to eradicate these HMs, such as chemical precipitation [8], adsorption [9] ion exchange [10], solvent extraction [11], and nano-filteration [12].

The HMs uptake by the adsorption mechanism depends on using an effective adsorbent for the exclusion of HMs from wastewater. K. Pawluk et al. [13] examined the effectiveness of the zeolite medium to eliminate Cu(II), Zn(II), Pb(II), Ni(II), and Cd(II) from aqueous solution. The results indicate that the percentage of removal was as follows: Zn(II) (92%), Pb(II) (70%), Cd(II) (54%), Ni(II) (48%), and Cu(II) (31%). Edris Bazrafshan et al. [14] used electrocoagulation for the removal of HMs from an aqueous environment containing Zn(II), Cu(II), Ni(II), Cr(III), Cd(II), and Hg(II). They found that the procedure is straightforward and instrument maneuver is uncomplicated.

Elfeky et al. [15] studied the obliteration of Cr(VI) from contaminated water employing a complex from Fe_3O_4 capped with cetyl-trimethyl-ammonium bromide (CTAB). The highest potency of the used system for the elimination of Cr(VI) (95.77%) was in the acidic medium (*p*H 4), contact time twelve h, and adsorbent quantity twelve mg/mL. The obtained results indicate that the Fe_3O_4/CTAB scheme demonstrated high potential and selectivity for managing water contaminated with Cr(VI).

Liliana Giraldo et al. [16] used Fe_3O_4 nanoparticles for the remedy of artificial aqueous solutions polluted by metal ions, such as Pb(II), Cu(II), Zn(II), and Mn(II). Results indicated that the adsorption capacity of Fe_3O_4 nanoparticles is utmost for Pb(II) and lowest for Mn(II), because of the diverse electrostatic attraction between HMs cations and negatively charged adsorption sites. The experimental results also illustrated that the adsorption is inclined by *p*H and temperature. F.I. El-Dib et al. [17] prepared magnetite nanoparticles and studied their adsorption properties for HMs within the presence of various synthesized surfactants. They found that the adsorption reaches equilibrium in four h and is significantly afflicted by the *p*H of the solution and the adsorbent amount. The adsorption performance is normalized by Langmuir adsorption isotherms.

A. M. Badruddoza et al. [18] tested Carboxymethyl-β-cyclodextrin/ Fe_3O_4 as nano-adsorbents for the exclusion of Cu(II). They found that the adsorption equilibrium is attained in 30 min and the adsorption kinetics of Cu(II) is found to follow a pseudo-second-order kinetic model. Equilibrium data for Cu(II) adsorption are fitted well by the Langmuir isotherm model. The highest adsorption capacity for Cu(II) ions is anticipated to be 47.2 mg/g at 25°C.

Amir Abdolmaleki et al. [19] examined triazinyl-β-cyclodextrin tailored Fe_3O_4 (T-β-CD–MNPs) for the elimination of HMs ions from aqueous solutions. Equilibrium results demonstrated that the HMs ion adsorption fit well with the Langmuir isotherm model, with the highest adsorption capacities of 105.38, 58.44, 51.30, and 33.33 mg/g for Pb(II), Cu(II), Zn(II), and Co(II), respectively.

Ahmed Fawzy El-Kafrawy et al. [20] used magnetic nano-adsorbent consisting of Fe_3O_4 nanoparticles tailored with CM-β-CD and PEG-β-CD. These magnetic nano-adsorbents were tested to efficiently eradicate Cu(II) and Pb(II) from contaminated samples. They reported that CD customized with PEG is more proficient than those adapted with carboxymethyl since the metal kinship to the PEG chain is superior to the metal kinship to the carboxymethyl group.

Polymers tailored nanoscale iron particles are an efficient selective sorbent for Pb(II), Zn(II) [21,22], and Ni(II) ions [23]. Nano-sized magnetic polymer adsorbent combined with tetraethylene-pentamine (TEPA-NMP) was developed for batch adsorption of Cr(VI) [24]. While Fe/Cu bimetallic adsorbent introduced as a novel industrial wastewater pre-management [25] and co-precipitation techniques [26] used for the elimination of Ni(II), Cr(VI), Cd(II), Mn(II), Pb(II), and Zn(II) with the aid of Cu(II) cyclohexyl methyl dithiocarbamate [27,28]. Natural polymers are preferred in modifying the nanoparticles surface to avoid cytotoxicity. Among natural polymers, cyclodextrin (CD) is considered a nontoxic polymer as it is composed of cyclic oligosaccharides. It can be used as a chelating agent to eradicate hazardous materials [29].

The pickling process in the steel industry releases high concentrations from hydrochloric acid iron waste (mainly in the form of $FeCl_2$). The discharge of this waste into a stream kills the fish due to the depletion of dissolved oxygen through the oxidation of iron. Thus, the disposal of such wastes is an important issue that may be solved through treatment protocols [30].

This study aims to recycle iron contaminated in the steel industry waste acid to highly valuable magnetic nanomaterials that can be modified by natural polymer (CD) and used for the removal of toxic HMs from contaminated wastewater. To the best of our knowledge, this is the first time that recycling of steel industry waste acid for wastewater treatment was described.

2. Materials and methods

2.1. Reagents

β-Cyclodextrin (98%) was purchased from Winlab-UK. Ammonium hydroxide (25%), and Hydrogen peroxide H_2O_2 (30%) were obtained from LOBA Chemie-India. Sodium hydroxide NaOH (99.9%), Monochloroacetic acid (≥99.0%), Hydrochloric acid HCl (37%), Cadmium nitrate $Cd(NO_3)_2.4H_2O$, Lead nitrate $Pb(NO_3)_2$, and potassium dichromate ($K_2Cr_2O_7$) were ordered from Sigma-Aldrich Chemical Co-USA. Epichlorohydrin (≥99.0%), Fe (iron (III) nitrate in nitric acid 0.5 mol/L, and Iron standard solution 1000 mg/L were bought from Scharlau-Spain. All chemicals were of analytical grade and used without additional purification. Waste hydrochloric acid was taken from Kandil steel waste acid station, industrial zone, Obour city, Block 13035 – PO, box 111 (Galvametal), Cairo, Egypt.

2.2. Synthesis of Carboxymethyl-β-Cyclodextrin (CM–β–CD) polymer

CM–β–CD polymer was synthesized according to the steps described in [31]. 5 g from β–Cyclodextrin was put in 50 mL from 10% (w/v) NaOH with constant stirring till they are mixed. Then, 10 mL from Epichlorohydrin was added gradually with intensive stirring for 8 h. Another 5 mL from Epichlorohydrin was added with continuous stirring for an additional 3 h. The mixture was lifted overnight at room temperature, then concentrated to 15 mL. The gummy precipitate was grown after vigorous stirring and washed 4 times with cold free ethanol. The precipitate was toughened after it was cleansed another time with cold acetone. Consequently, a high pure yield of β-CD/Epichlorohydrin copolymer of (80%) was gained. The next essential step for preparing the desired polymer was done by dissolving 4 g from β-CD/Epichlorohydrin copolymer in 100 mL of 5% (W/V) NaOH solution, and then 4 g Monochloroacetic acid was added gradually. The mix was strongly stirred for twenty-four h. To neutralizing the excess NaOH, 2M HCl was added drop by drop until the *p*H became neutral. The mixture was concentrated to15 mL and cooled over ice to 4°C. Salt crystals were generated by filtration. The polymer was precipitated by vigorous stirring with cold free ethanol, and washed 4 times with free ethanol thus, a high pure yield (55%) of CM–β–CD was obtained.

2.3. Preparation of CM-β-CD conjugated Fe_3O_4 nanocomposite (CM-β-CD/ Fe_3O_4)

1.5 g from synthesized CM–β–CD polymer was dissolved in 40 mL distilled water followed by the addition of 4.77 g from steel hydrochloric acid waste (see supporting information for calculation of Fe^{2+} or Fe^{+3} in the waste sample). Then, 15 mL NH4OH (25% V/V) was mixed gradually with polymer/waste mixture under vigorous stirring (161 xg) for one h at room temperature.

2.4. Preparation of HM samples for elemental analysis by atomic absorption spectrometer

The sample concentrations of 25,100,300 and 400 mg/L were prepared from nitrate salt of Pb(II), Cd(II), and potassium dichromate salt (containing Cr[VI]). Three standard solutions (5, 10, and 15 mg/L) for Pb(II), Cd(II), and Cr(VI) were also made. Adjusting the *p*H of the solution was done by standard solution from NaOH and HCl (0.1 N).

2.5. Studying the factors affecting adsorption of HMs ions by (CM-β-CD/Fe_3O_4) nanocomposite

The adsorption process is affected by many factors such as the pH of the solution, initial HMs concentration, contact time with the adsorbent, and the presence of other co-existing ions (interfering ions). In all studied factors, three sample replicates were done for each adsorption reaction. The sample volume was 10 mL using DI in all laboratory samples. The weight of the tested polymer (CM-β-CD/ Fe_3O_4) was 24 mg, *p*H 5.5, and the used HMs concentration of 300 mg/L with continuous stirring (14 xg) at room temperature (RT) 25C°.

2.5.1. Effect of *p*H value

Solutions pHs of 1.5, 3.5, 5.5, and 6.5 were prepared. 0.1 N solution from NaOH and HCl was used for adjusting *p*H values.

2.5.2. Effect of initial HMs concentration

Different concentrations of 25, 100, 200, 300, and 400 mg/L were prepared for the effect of initial HMs concentration study.

2.5.3. Effect of contact time

The reaction was performed at different times (every 10 min until 60 min then 120 min, 240 min, and 300 min).

2.5.4. Effect of interfering ions

The effect of different coexisting ions on the adsorption capacity of CM-β-CD/ Fe_3O_4 was examined by mixing the proposed HM samples in a binary (2 elements), ternary (3 elements), and quaternary (4 elements) mixture. The mixture solution for each HM was prepared by mixing equal volumes (10 mL) from every HM element solution. Concentrations of 300 mg/L from each HM were prepared for this study.

2.6. Field samples

The real field samples were collected from three industrial sewer zones at Cairo Governorate-Egypt, Kandil steel Galva metal at El Obour site (*p*H 3.1), Kafr Abyan sewer - Abu Zabal -Al Khanka (pH 7.1), Akracha sewer industrial zone at Abu Zabal -Al Khanka (*p*H 6.9). The real field experiments were performed using 24mg CM-β-CD/ Fe_3O_4 composite and 10 mL wastewater sample volume. The contact time was 5 h at a shaking rate of 14 xg. Then, the three HMs Cr(II), Cd(II), and Pb(II) concentrations were measured and the adsorption capacity was also calculated.

2.7. Reusability of the adsorbent

The reusability of the adsorbent was tested by a collection of CM-β-CD/ Fe_3O_4 using an external magnetic field then it was inserted in 10 mL of the contaminated sample for 1 h and shaking rate of 14 xg then the sample was taken for HMs analysis after adsorbent removal by magnetic collection. Desorption of the adsorbent was done by a collection of CM-β-CD/ Fe_3O_4 then insertion in 10 mL of 0.1 M Na2EDTA (37.22 g EDTA/L) [32]. After the desorption of HMs ions from CM-β-CD/ Fe_3O_4, it was washed and dried for reusing purposes.

2.8. Instruments

The infrared spectra (4000–399 cm^{-1}) were determined using an infrared spectrometer JASCO FT/IR-4100. X-ray diffraction (XRD) diffractometer PANalytical's X'Pert PRO with Cu Kα radiation was used to record the sample diffraction patterns. Images were taken by a transmission electron microscope (FEI Tecnai G2 20 200 KV TEM). The elemental analysis was performed by a Perkin-Elmer atomic absorption spectrophotometer (analyst 200, USA).

3.Results and discussions

Characterization of the prepared nanocomposite

FTIR spectrum in Figure 1 (a) displayed the characteristic peaks for β-cyclodextrin, bare magnetic nanoparticles Fe_3O_4, and composite product CM-β-CD/ Fe_3O_4. For unmodified Fe_3O_4 nanoparticles and composite nanoparticles, the distinctive absorption band of magnetite at 566 cm^{-1} is clearly detectable in the spectra [15]. Compared with bare magnetite nanoparticles, the prepared CM-β-CD/ Fe_3O_4 nanocomposite has newly emerged absorption bands at 1065, 1262, and 2936 cm^{-1} related to –CO, C–O–C, and C–H bonds in β-CD, respectively. This signifies that the β-CD molecule has been joined with magnetite nanoparticles efficiently. In Figure 1a (CM-β-CD/ Fe_3O_4), the peak at 1615cm^{-1} corresponds to the carbonyl (C=O) of the carboxymethyl group (–$COOCH_3$) in CM–β–CD. This band intensity was reduced compared with that of normal carbonyl in β-cyclodextrin due to the interaction of the carbonyl group with the iron oxide nanoparticles, resulting in the formation of the iron oxide nanoparticles capped with carboxylate [18].

The XRD pattern (Figure 1b) of Fe_3O_4 NPs and for CM-β-CD/ Fe_3O_4 indicates a highly crystalline cubic structure of Fe_3O_4 nanoparticles at the diffraction peaks of 30.1, 35.5,43.3, 53.6, 57.0, and 232 62.6°, which correspond to D220, D311, D400, D422, D511, and D440 planes of the cubic Fe_3O_4 lattice, respectively. These results are in good conformity with the XRD patterns of Fe_3O_4 NPs reported in previous literature [33,34], which proved that the cubic spinel construction of the magnetite nanoparticles with a crystal size of about 17.02 nm. XRD pattern for CM-β-CD/ Fe_3O_4 polymer has diffraction peaks at 14.09, 27.0, 30.0, 35.4, 43.3, 46.8, 57.0, and 62.6° correspond to D020, D120, D011, D031, D060, D200, D151, and D251 respectively for planes of the orthorhombic crystal. The crystallite size of the sample was calculated from peaks using the Debye–Scherrer formula [35]. The calculated size was 83 nm for composite CM-β-CD/ Fe_3O_4 and 12 nm for bare Fe_3O_4. TEM images Figure 1 (c) illustrates (I) bare magnetic nanoparticles (Fe_3O_4) and (II) synthesized nanocomposites CM-β-CD/ Fe_3O_4.

From Figure 1c it can be seen that the bare magnetite nanoparticles (Figure 1-c [I]) are approximately 10–15 nm in diameter and tend to agglomerate. The square-like shapes represent the cubic crystals. The better distribution state of the composite nanoparticles can be observed from Figure 1c(II) with a range of diameters from 72 to 102 nm, which is comparable with the average size calculated from XRD data (83 nm). The composite nanoparticles display approximately spherical shapes resembling a core-shell structure. The core-shell structure consists of multiple magnetite cores and an outer layer of CM-β-CD polymer (Figure 1-c [II]).

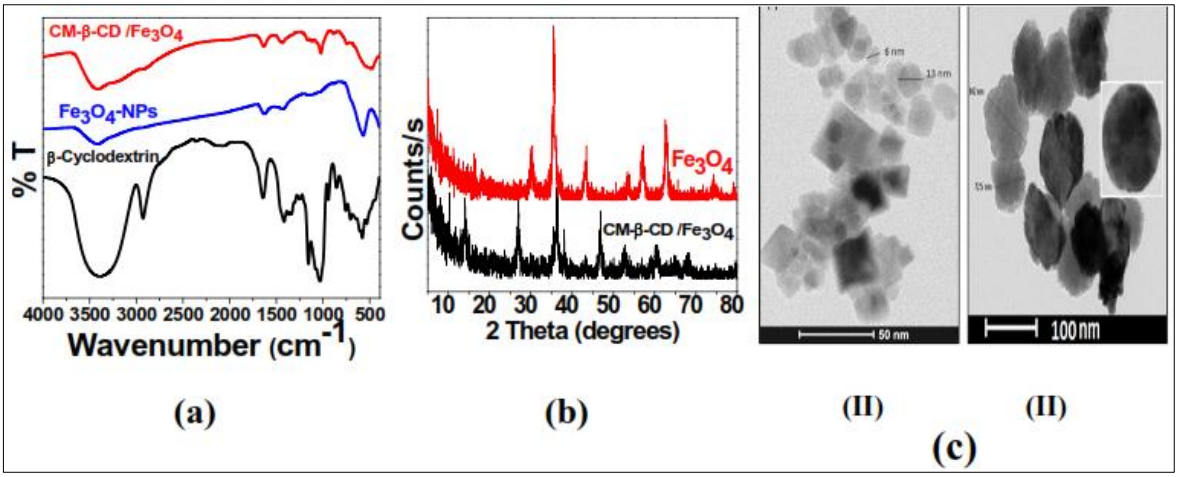

Figure 1. (a) FTIR spectra for β-Cyclodextrin, Fe_3O_4-NPs, and CM-β-CD /Fe_3O_4 Nanocomposite (b) XRD patterns for the prepared Fe_3O_4-NPs, and CM-β-CD /Fe_3O_4 (c) TEM images of (I) bare magnetic nanoparticles (Fe_3O_4) and (II) synthesized nanocomposite CM-β-CD /Fe_3O_4 at two magnifications

Factors affecting the adsorption process

Many conditions controlling the adsorption of the HMs, especially the initial concentration of HM, the *p*H of the solution, the contact time between HM and adsorbent, and the existence of other competing ions in the solution.

HMs initial concentration was tested as an effective factor in the adsorption of HMs onto adsorbents. Eq. (1) was used for calculating % removal [15].

$$\%\ Removal\ \frac{C_0 - C_f}{C_0} \times 100 \quad (1)$$

where C0 and Cf are the initial and final concentrations of HMs in the solution, respectively.

According to Figure 2 (a), the % removal increases with increasing initial HMs concentration and it was in the order of Pb(II)>Cd(II)>Cr(VI).

Figure 2(a) suggests that the adsorption affinity of CM-β-CD/ Fe_3O_4 nanocomposite was highest toward Pb(II) while it was lowest for Cr(VI) irrespective of their initial concentration.

A previous study revealed that sorption is directly proportional to the molar mass and metal ionic radii [36]. Thus, CM-β-CD/ Fe_3O_4 sorption efficiency was in the order of Pb(II) 1.19 Å> Cd(II) 0.95 Å> Cr(VI)0.58 Å.

The *p*H of the aqueous solution is a vital factor in the adsorption process. Thus, to understand the effect of *p*H on the sorption of HMs ions on CM-β-CD/ Fe_3O_4, a *p*H range of 1.5–6.5 was investigated in this study. Precipitation of HMs as metal hydroxide would happen at *p*H greater than 6.5, therefore the test was terminated at *p*H 6.5. The effect of *p*H on the adsorption capacity is plotted in Figure 2(b). The adsorption capacity was calculated according to Eq. (2) [37].

$$Qe = \frac{C_0 - C_e}{W} \times V \quad (2)$$

where Qe is the equilibrium adsorption capacity of the adsorbent in mg (metal)/g (adsorbent), C0 is the concentration of metal ions before adsorption in mg/L, Ce is the equilibrium concentration of metal ions in mg/L (remained in solution after shaking), V is the volume of metal ion solution in liter scale, and W is the weight of the adsorbent in gram scale. The concentration of HMs in the supernatant was determined by flame atomic absorption spectroscopy [38].

The effect of *p*H can be elucidated by considering the surface charge of the adsorbent material. Metals aqueous solution has positive zeta potential at *p*H < 7. Since the zeta potentials of the CM-β-CD/ Fe_3O_4 are positive at *p*H < 4.7 (point of zero charge, pzc) [18], it is assumed that the interactions between the adsorption sites (multiple hydroxyl and carboxyl groups) on CM-β-CD/Fe_3O_4 and HM ions are electrostatically repulsive for Cd(II), and Pb(II) and attractive to Cr(VI). Above *p*H 4.7, the reverse should happen. However, as seen in Figure 2(b) this expected behavior does not occur. Conversely, the adsorption capacity remains constant regardless of the *p*H value. These results imply that the electrostatic interaction is not the key factor that affects the adsorption and metal chelation plays a much more important role [39].

To test the effect of contact time on the adsorption efficiency of CM-β-CD/ Fe_3O_4, the reaction was performed at different contact times (0–360 min). The results of adsorption capacity are plotted in Figure 2c.

As the contact time increases the adsorption rate increased until it reached equilibrium in 60 min. Therefore, CM-β-CD/ Fe_3O_4 could be easily and rapidly adsorb HMs as Cr(VI), Cd(II), and Pb(II). At that time, the adsorption capacity of CM-β-CD/ Fe_3O_4 was 64.2 (mg/g) for Pb(II), 31.6 (mg/g) for Cd(II), and 10.2 (mg/g) for Cr(VI). Accordingly, the analysis of kinetic curves for each metal could arrange them as Pb(II)> Cd(II)>Cr(VI) because of the increased ion exchange rate, which depends on their ionic radii [36].

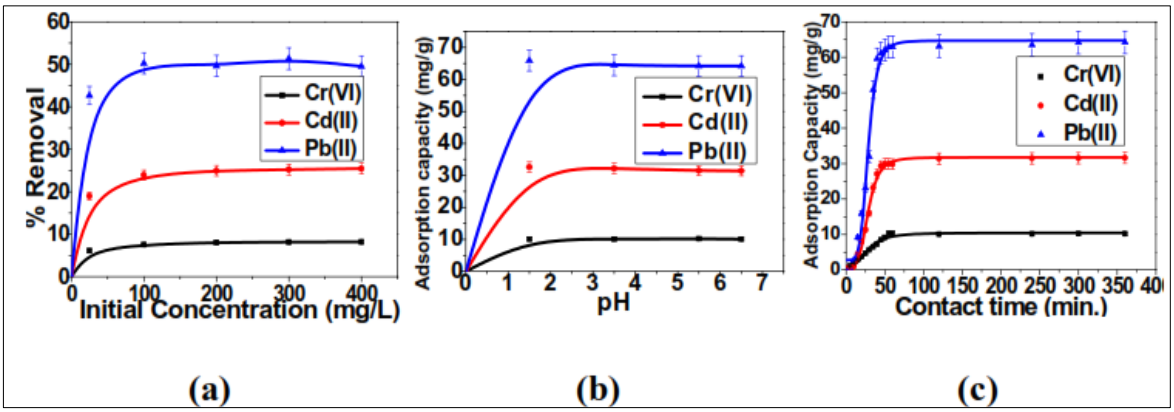

Figure 2. Effect of (a) different HMs initial concentration at *p*H 5.5 and contact time 1h, (b) different *p*H values at contact time1h and HMs initial concentration of 300 mg/L, and (c) different contact times at *p*H 5.5 and HMs initial concentration of 300 mg/L on CM-β-CD /Fe_3O_4 adsorption capacity (Q_e) at RT

Adsorption kinetic study

The adsorption mechanism of metals can be investigated by employing the pseudo-first-order and pseudo-second-order kinetic models. The pseudo-first-order kinetic model (see supporting information) adopts that the binding originates from physical adsorption [40]. While the pseudo-second-order kinetic model (see supporting information) is based on chemical adsorption (chemisorption) [15].

From Figure 3, it appears that the second-order model seems to be more favorable for HMs sorption process, indicates their chemisorption by CM-β-CD/ Fe_3O_4 nanocomposite.

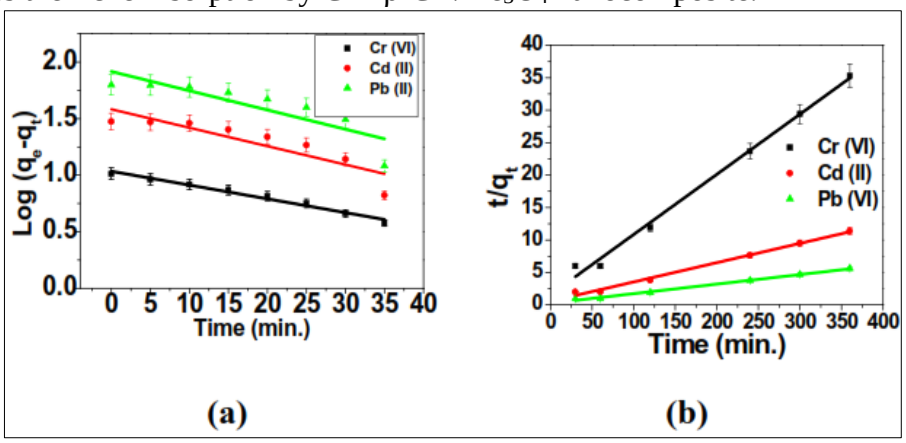

Figure 3. The plot of (a) pseudo-first-order and (b) pseudo-second-order models for the sorption of HM from a contaminated sample using CM-β-CD /Fe_3O_4 nanocomposite

The parameters obtained from the linear fitting of pseudo-first-order and pseudo-second-order models for CM-β-CD/ Fe_3O_4 are listed in Table 1.

Table 1. Parameters of kinetic models for the sorption of HMs by CM-β-CD/Fe_3O_4 nanocomposite

	Pseudo-first order		Pseudo-second order		
Metal	K_1	R^2	K_2	Qe(mg/g)	R^2
Cr (VI)	0.033	0.977	7.970	10.145	0.992
Cd (II)	0.030	0.760	2.610	31.500	0.991
Pb (II)	0.045	0.768	1.239	63.753	0.992

The table illustrates that the correlation coefficient (R2) for the pseudo-second-order adsorption model has high values for all HMs compared with that of the pseudo-first-order model. Accordingly, the adsorption mechanism is chemisorption due to more fitting to the pseudo-second-order model. The pseudo-second-order adsorption has also been reported for kinetics of adsorption of Cu(II) using Carboxymethyl-β-cyclodextrin conjugated Fe_3O_4 [18].

Adsorption isotherm study

The common adsorption isotherm models (Langmuir and Freundlich) were used to describe the adsorption of Pb (II), Cd (II), and Cr (VI) on CM-β-CD/ Fe_3O_4 nanocomposite. The Langmuir model (supporting information) assumes that all adsorption sites of the adsorbent have identical binding energy and each site binds to only a single adsorbate (one layer of molecules can be adsorbed on the surface) [41].

While the Freundlich model (supporting information) is based on the reversible heterogeneous adsorption [41].

Figure 4 proved that the adsorption of Pb(II), Cd(II), and Cr(VI) on CM-β-CD/ Fe_3O_4 are fitted more with the Langmuir model (a) than the Freundlich model (b).

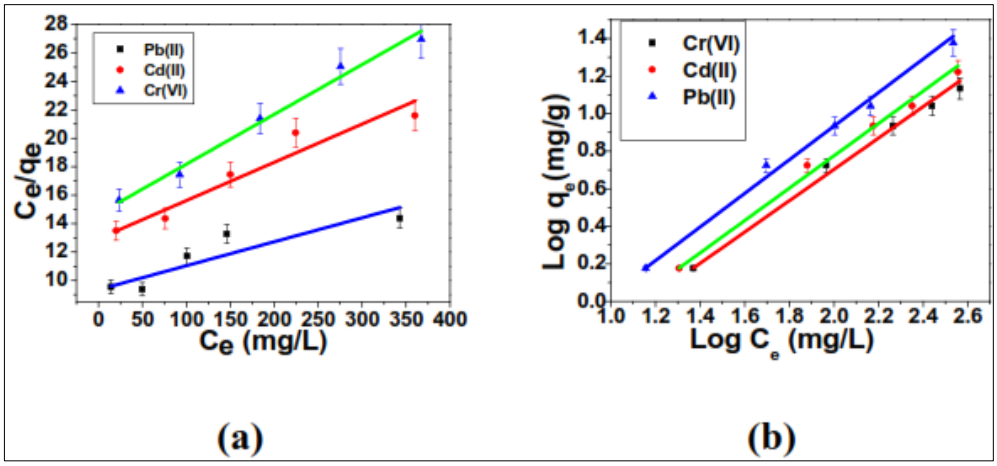

Figure 4. Adsorption isotherm of Pb(II), Cd(II), and Cr(VI) on CM-β-CD /Fe_3O_4 plotted by (a) Langmuir model, and (b) Freundlich model

The parameters for both models are presented in Table 2.

Table 2. Freundlich and Langmuir isotherm parameters for the adsorption of HMs on CM-β-CD /Fe_3O_4 nanocomposite

	Langmuir model			*The Freundlich model*		
Metal	q_m(mg/g)	K_L(1/mg)	R^2	n	K_f	R^2
Cr (VI)	10.2	0.0024	0.9835	16	5.719	0.9588
Cd (II)	31.5	0.0033	0.9682	21	6.696	0.8961
Pb (II)	64.2	0.0039	0.9351	24	8.114	0.9341

Usually, for evaluating a good fit, values of correlation coefficients (R^2) of linear plots of the two models are compared. From Table 2, the correlation coefficient (R^2) is higher in the case of applying the Langmuir model than the Freundlich model.

The effect of interfering ions

HMs waste always contains a mixture of different metal ions that may affect the adsorption efficiency of each other. Table 3 shows the percentage removal results of each metal ion in a binary system (a), the

ternary system (b), and quaternary system (c) calculated relative to percentage removal in a single system. The results presented in Table 3 suggest that the interfering ions in most cases do not significantly affect the percentage removal of the measured metal ion. Similar results were obtained by [15] when Fe_3O_4/ CTAB was used for Cr(VI) removal. Thus, the CM-β-CD/ Fe_3O_4 can be used efficiently in a multi-component system.

Table 3. Removal percentage of HMs in a multi-component system: binary, ternary, and quaternary calculated relative to percentage removal in a single system using CM-β-CD/Fe_3O_4 nanocomposite adsorbent

a-Binary system	%Removal	SD	RSD
Cr*+Cd	98.46%	0.020	0.216
Cr*+Pb	98.91%	0.020	0.307
Cd*+Pb	96.23%	0.276	1.220
Cd*+Cr	95.63%	0.046	0.175
Pb*+Cd	98.03%	2.860	24.165
Pb*+Cr	99.96%	0.143	63.019
b- Ternary system			
Cr*+Pb+Cd	99.19%	0.020	0.275
Cd*+Cr+Pb	97.43%	0.286	1.237
Pb*+Cd+Cr	99.96%	0.024	6.614
c- Quaternary system			
Cr *+Pb+Cd+ Ni	96.98%	0.656	1.811
Cd*+Pb+Cr+Ni	97.94%	0.458	1.849
Pb*+Cd+Cr+Ni	100.%	0.480	117.704

** The measured HM ion from the mixture.*

Reusability of CM-β-CD/ Fe_3O_4

In this study, CM-β-CD/ Fe_3O_4 composite was reused for four successive cycles in contaminated samples. The HMs removal was measured by atomic absorption spectrophotometer. The adsorption capacity ratio percentage was calculated according to Eq. (3).

$$R_e = \frac{Q_r}{Q_o} \times 100(\%) \quad (3)$$

where Re is the adsorption capacity ratio %, Qo is the adsorption capacity of CM-β-CD/ Fe_3O_4 in mg (metal)/g (adsorbent) in the first cycle, and Qr is the adsorption capacity of CM-β-CD/ Fe_3O_4 in mg (metal)/g (adsorbent) at the second, third or fourth cycle. Figure 5 shows the adsorption capacity ratio percentage of Pb(II), Cd(II), and Cr (VI) using CM-β-CD/ Fe_3O_4 for four successive cycles. The figure illustrates that the adsorption capacity ratio percentage of CM-β-CD/ Fe_3O_4 does not significantly change in the four cycles. This may be due to maintaining the magnetic properties and composite reactivity by the encapsulating polymer CM-β-CD. Approximately comparable results were reported by Hu et al. [42] who found that β-cyclo-dextrin attached MWC-NTs/iron oxides/CD can be reused five times for Pb(II) adsorption with less than 5% of reduction in efficiency, signifying the high quality of the adsorbents. This study recyclability results propose that CM-β-CD/ Fe_3O_4 nano-adsorbents can be repetitively used as a proficient adsorbent in wastewater treatment.

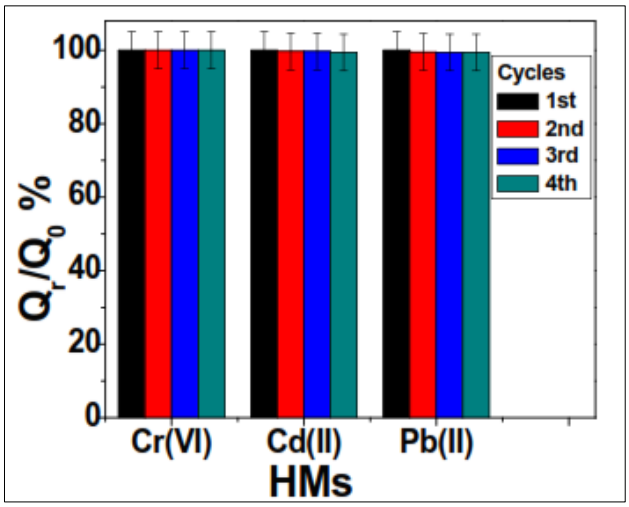

Figure 5. CM-β-CD/Fe_3O_4 adsorption capacity rate percentagein mg (metal)/g (adsorbent) for Cr (VI), Cd(II) and Pb(II) for 4 successive adsorption cycles

Wastewater Field sample test

The real field samples were collected from three industrial sewer zones at Cairo Governorate-Egypt, Sample (1) from Kandil steel Galva metal (*p*H 3.1), sample (2) from Kafr Abyan sewer (*p*H 7.1), and sample (3) from Akracha sewer (*p*H 6.9). The real field experiments were performed applying the same parameters of laboratory sample testing. Table 4 shows the percent removal of Pb(II), Cd(II), and Cr (VI) from the three field industrial sewer samples using CM-β-CD/Fe_3O_4 (24 mg) adsorbent applying Eq. (1).

Table 4. Removal percentage of HMs in field samples using CM-β-CD/Fe_3O_4 nanocomposite adsorbent

Sample	Cr (VI)			Cd(II)			Pb(II)		
	C_0 (mg/L)	C_f (mg/L)	*% Removal*	C_0 (mg/L)	C_f (mg/L)	*% Removal*	C_0 (mg/L)	C_f (mg/L)	*% Removal*
(1)	6.6	0.08	98.8%	0.42	0.009	97.9%	1.22	0.014	98.9%
(2)	9.6	0.1	99.0%	0.6	0.01	98.3%	0.82	0.007	99.1%
(3)	16.7	0.19	98.9%	0.3	0.003	99.0%	1.19	0.01	99.2%

As viewed in the results the efficiency of the synthesized polymer is high, as the percentage removal is more than 97% in all tested HM field samples.

4. Conclusions

The CM-β-CD/ Fe_3O_4 nanocomposite was synthesized by one step (co-polymerization) reaction. TEM and XRD revealed that CM-β-CD/ Fe_3O_4 size was approximately 80 nm. FTIR illustrated the interaction of the carbonyl group in CM-β-CD with the Fe_3O_4 nanoparticles resulting in the formation of the CM-β-CD/ Fe_3O_4. The adsorption results illustrated that CM-β-CD/ Fe_3O_4 sorption is directly proportional to the molar mass and metal ionic radii. The adsorption equilibrium of HMs was reached at 1h. The maximum adsorption was for Pb(II) at an initial concentration of 300 mg/L, *p*H 5.5, and contact time 1 h. Kinetic study results indicated that HMs were chemically absorbed by CM-β-CD/ Fe_3O_4 nanocomposite. From equilibrium modeling, the results of HMs adsorption are more fitting to the Langmuir model than the Freundlich model. The interfering ions and recyclability of the adsorbent do not significantly affect the percentage removal of the measured metal ion. The synthesized polymer proved a high success and stability in the field applications. Thus the CM-β-CD/ Fe_3O_4 can be used

efficiently for wastewater purification with high efficiency and good recyclability due to maintaining the magnetic properties and composite reactivity by the encapsulating polymer CM-β-CD. Future studies will focus on enfolding the CM-β-CD/ Fe_3O_4 in a filter with different natural polymers.

Acknowledgment.This work was supported by the National Institute of Laser Enhanced Sciences (NILES), and Faculty of Science. Cairo University-Egypt. The authors would also like to express the deepest appreciation for Kandil Steel Company (Qalubiya-Egypt), R&D, and Chemistry team for the help and support.

References

1.GABRIEL B. Part E: The fate and toxicity of chemicals in wastewater treatment plants in Wastewater microbiology. 3rd Ed. New Jersey; 2005. P. 499-527.
2.SHARMA PD. Environmental Biology, 2nd Ed. Rastogi publication India; 2008.
3.PAY D, CHRISTOPHER AS, LIQA R-S, MARK R, AKICA B. Wastewater Irrigation and Health: Assessing and Mitigating Risk in Low-income Countries. Earthscan, Routledge UK; 2009
4.B.A. RYBICKI M.H.S, C.C JOHNSON, J. UMAN, J.M. GORELL, Parkinson's disease mortality and the industrial use of heavy metals in Michigan, Mov. disord. 8:1 (1993) 87-92.
doi: 10.1002/mds.870080116
5.J.M.MATÉS, J.A.SEGURA, F.J.ALONSO. J.MÁRQUEZ, Roles of dioxins and heavy metals in cancer and neurological diseases using ROS-mediated mechanisms, Free Radic. Biol. Med. 49:9 (2010) 1328-1341. doi: 10.1016
6.P.E. BIGAZZI, Autoimmunity and heavy metals, Lupus 3:6 (1994) 449-453.
doi:10.1177/096120339400300604.
7.S. AGARWAL, T. ZAMAN, E.M. TUZCU, S.R. KAPADIA, Heavy metals and cardiovascular disease: Results from the National Health and Nutrition Examination Survey (NHANES) 1999-2006, Angiology 62:5 (2011) 422-429. doi:10.1177/0003319710395562.
8.O.D. ULUOZLU, M. TUZEN, D. MENDIL, M. SOYLAK, Coprecipitation of trace elements with Ni^{2+}/2-nitroso-1-naphthol-4 sulfonic acid and their determination by flame atomic absorption spectrometry, J. Hazard. Mater. 176 (1-3) (2010) 1032−1037. doi:10.1016/j.jhazmat.2009.11.144.
9.SARKAR S, ADHIKARI S. Adsorption technique for removal of heavy metals from water and possible application in wastewater-fed aquaculture. In: Jana B, Mandal R, Jayasankar P. Wastewater management through aquaculture. Springer nature Singapore; 2018. P. 235-251
10.I. KOYUNCU, N. AKCIN, G. AKCIN, K.F. MUTLU, Comparative study of ion-exchange and flotation processes for the removal of Cu^{2+} and Pb^{2+} ions from natural waters, Rev. Anal. Chem. 29 (2010) 93−106. doi:10.1515/REVAC.2010.29.2.93.
11.A.B RESTERNA, R. CIERPISZEWSKI, K. PROCHASKA, Kinetic and equilibrium studies of the removal of cadmium ions from acidic chloride solutions by hydrophobic pyridinecarboxamide extractants, J. Hazard. Mater. 179 (1-3) (2010), 828−833. doi:10.1016/jhazmat.2010.03.078.
12.L.B. CHAUDHARI, Z.V. MURTHY, Separation of Cd and Ni from multicomponent aqueous solutions by nanofiltration and characterization of membrane using IT model, J. Hazard. Mater. 180 (1-3) (2010), 309−315. doi: 10.1016/j.jhazmat.2010.04.032.
13.K. PAWLUK, J. FRONCZYK, K. GARBULEWSKI, Removal of dissolved metals from road runoff using zeolite PRBs, Chem. Eng. Trans. 32 (2013) 331–336. doi:10.3303/CET1332056.
14.E. BAZRAFSHAN, L. MOHAMMADI, A. ANSARI-MOGHADDAM, A.H. MAHVI, Heavy metals removal from aqueous environments by electrocoagulation process– a systematic review, J. Environ. Health Sci. Eng. 13:47 (2015) 1-16. doi: 10.1186/s40201-015-0233-8.
15.S.A. ELFEKY, S.E. MAHMOUD , A.F. YOUSSEF, Applications of CTAB modified magnetic nanoparticles for removal of chromium (VI) from contaminated water, J. Adv. Res. 8:4 (2017) 435–443. doi: 10.1016/j.jare.2017.06.002.

16. L. GIRALDO, A. ERTO, J.C. MORENO-PIRAJA, Magnetite nanoparticles for removal of heavy metals from aqueous solutions: Synthesis and characterization, Adsorption 19 (2013) 465–474. doi: 10.1007/s10450-012-9468-1
17.F.I. EL-DIB, D.E. MOHAMED, O.A. EL-SHAMY, M.R. MISHRIF MR, Study the adsorption properties of magnetite nanoparticles in the presence of different synthesized surfactants for heavy metal ions removal, Egypt. J. Pet. (2020). https://doi.org/10.1016/j.ejpe.2019.08.004.
18.A.Z. BADRUDDOZA, A.S. TAY, P.Y.TAN, K. HIDAJAT, M.S. UDDIN, Carboxymethyl-β-cyclodextrin conjugated magnetic nanoparticles as nano-adsorbents for removal of copper ions: Synthesis and adsorption studies, J. Hazard. Mater. 185 (2–3) (2011) 1177-1186. doi:10.1016/j.jhazmat.2010.10.029.
19.F. PAQUIN, J. RIVNAY, A.SALLEO, N. STINGELIN, C. SILVA-ACUNA, Multi-phase semi-crystalline micro-structures drive exciton dissociation in neat plastic semiconductors, J. Mater. Chem. C. 3 (2015) 10715-10722. doi:10.1039/b000000x.
20.A.F. EL-KAFRAWY, S.M. EL-SAEED, R.K. FARAG, H.A. EL-SAIED, M.E. ABDEL-RAOUF, Adsorbents based on natural polymers for removal of some heavy metals from aqueous solution, Egypt. J. Pet. 26:1 (2017):23-32. doi:10.1016/j.ejpe.2016.02.007.
21.Z. CHENG, A.K. TAN, Y. TAO, D. SHAN, K.E. TING, X.J. YIN, Synthesis and characterization of iron oxide nanoparticles and applications in the removal of heavy metals from industrial wastewater, Int. J. Photoenergy, (2012), art. no. 608298:1-5. doi:10.1155/2012/608298.
22. K.R. SIDHAARTH, J. JEYANTHI, N. NARAYANAN, Comparative studies of removal of lead and zinc from industrial wastewater and aqueous solution by iron oxide nanoparticles: Performance and mechanisms, European Journal of Scientific Research, 70:2 (2012) 169-184.
23.A.Z. BADRUDDOZA, Z.B. SHAWN, W.J. TAY, K. HIDAJAT, M.S. UDDIN, Fe_3O_4/cyclodextrin polymer nanocomposites for selective heavy metals removal from industrial wastewater, Carbohydr. Polym. 91:1 (2013) 322-332. doi:10.1016/j.carbpol.2012.08.030.
24.Y.G. ZHAO, H.Y. SHEN, M.Q. HU, F. WEI, Y.J. LUO, Q.H. XIA, Synthesis of NH2-Functionalized Nano-Fe_3O_4 Magnetic Polymer Adsorbent and its Application for the Removal of Cr (VI) from IndustrialWastewater. Adv. Mat. Res. 79-82 (2009) 1883-1886. doi: 10.4028/www.scientific.net/amr.79-82.1883.
25. X. LIU, H.W. WANG, J. H. FAN, L. M. MA, J. XU, An engineering practice of industrial wastewater treatment with Fe/Cu bimetallic process, Applied Mechanics and Materials 694 (2014) 396-405. doi:10.4028/www.scientific.net/amm.694.396.
26.J.A. OTERO, O. MAZARRASA, A. OTERO-FERNANDEZ, M.D. FERNÁNDEZ, A. HERNÁNDEZ, A .MAROTO - VALIENTE, Treatment of wastewater. Removal of heavy metals by nanofiltration. Case study: Use of TFC membranes to separate Cr (VI) in industrial pilot plant, Procedia Engineering 44 (2012) 2020-2022. doi:10.1016/j.proeng.2012.09.029.
27.S.A. NOSIER, Removal of cadmium ions from industrial wastewater by cementation, Chem. Biochem. Eng. Q. 17:3 (2003) 219-224.
28. O.E. ABDEL-SALAM, I.M. ISMAIL, A. SOLIMAN, A.A. AFIFY, H.M. ALY, Removal of lead from industrial wastewater using flow-by-porous electrode, Port. Electrochim. Acta 32:1 (2014) 65-75 doi:10.4152/pea.201401065.
29. E.M. DEL VALLE, Cyclodextrins and their uses: a review, Process Biochem. 39:9(2004) 1033-1046. doi: 10.1016/s0032-9592(03)00258-9.
30.S.E. COBURN, Disposal of acid-iron wastes from a steel mill, Ind. Eng. Chem. 20:3 (1928) 248-249. doi: 10.1021/ie50219a011.
31.M. FERNÁNDEZ, M.L. VILLALONGA, A. FRAGOSO, R. CAO, M. BAÑOS, R. VILLALONGA, α-Chymotrypsin stabilization by chemical conjugation with O-carboxymethyl-poly-β- cyclodextrin, Process Biochem. 39:5 (2004) 535-539. doi: 10.1016/S0032-9592(03)000694.

32.S. LATA, P.K. SINGH, S.R. SAMADDER, Regeneration of adsorbents and recovery of heavy metals: a review, Int. J Environ. Sci. Technol. 12:4 (2015) 1461-1478. doi:10.1007/s13762-014-0714-9.
33. S. SUN, H. ZENG, D.B. ROBINSON, S. RAOUX. P.M. RICE, S.X. WANG, et al., Monodisperse MFe_2O_4 (M = Fe, Co, Mn) nanoparticles, J. Am. Chem. Soc. 126:1 (2004) 273-279. doi: 10.1021/ja0380852.
34. L.A. HARRIS, J.D. GOFF, A.Y. CARMICHAEL, J.S. RIFFLE, J.J. HARBURN, T.G. PIERRE, et al., Magnetite nanoparticle dispersions stabilized with triblock copolymers, Chem. Mater. 15:6 (2003) 1367-1377. doi: 10.1021/cm020994n.
35.AZAOFF LV. Elements of X-ray crystallography. McGraw-Hill Book Co: New York; 1968.
36.M. FRANUS, L. BANDURA, Sorption of heavy metal ions from aqueous solution by glauconte, Fresenius Environ. Bull. 23 (2014) by PSP No. 3a.
37. J. SONG, H. KONG, J, JANG. Adsorption of heavy metal ions from aqueous solution by poly rhodanine-encapsulated magnetic nanoparticles, J. Colloid Interf. Sci. 359:2(2011) 505–511. doi:10.1016/j.jcis.2011.04.034.
38.S.V. KUMAR, R. NARAYANASWAMY, M. SRIPATHY, K.V. PAI, Comparative study of removal of chromium (VI) ion from aqueous solution using eucalyptus, neem and mango leaves, Int. J. Eng. Res. Dev. 8:2 (2013) 56–61. www. Ijerd.com.
39. Y. XIAO, H. LIANG, W. CHEN, Z. WANG, synthesis and adsorption behavior of chitosan-coated mnfe2o4 nanoparticles for trace heavy metal ions removal, appl. Surf. Sci. 285p (2013) 498–504. Doi: 10.1016/j.apsusc.2013.08.083.
40.F-C. WU, R-L. TSENG, R-S. JUANG, kinetic modeling of liquid-phase adsorption of reactive dyes and metal ions on chitosan, water res. 35:3 (2001) 613–618. Doi: 10.1016/s0043-1354(00)00307-9.
41.S.A. BHATT, L.P. SAKARIA, M. VASUDEVAN, R.R. PAWAR, N. SUDHEESH, C.H. BAJAJ, et al, adsorption of an anionic dye from aqueous medium by organoclays: equilibrium modeling, kinetic and thermodynamic exploration, rsc adv. 2 (2012) 8663–8671. Doi:10.1039/c2ra20347b.
42. J. HU, D. SHAO, C. CHEN, G. SHENG, J. LI, X. WANG, M. NAGATSU, Plasma-induced grafting of cyclodextrin onto multiwall carbon nanotube/iron oxides for adsorbent application, J. Phys. Chem. B 114 (2010) 6779–6785. doi: 10.1021/jp911424k.

Manuscript received: 31.10.2020